

Template-free synthesis and characterization of leaf-like Fe-Ni microstructures

Yang Cao¹, Shi Gang Ai², Jinglin Zhang^{1*}, Ning Gu¹, Shuangqi Hu¹

¹Department of Chemistry Engineering, North University of China, Taiyuan 030051, P.R. China

²College of engineering, Peking University, Beijing 100871, P.R. China

*Corresponding authors. Tel: (+86) 351-3557256; E-mail: syyi@pku.edu.cn

Received: 30 June 2012, Revised: 27 August 2012 and Accepted: 01 September 2012

ABSTRACT

Leaf-like Fe-Ni alloy have been synthesized via a facile hydrothermal approach without any soft and hard template. The structure of the leaf-like Fe-Ni alloy was characterized by Scanning electron microscopy (SEM), X-ray diffraction (XRD) and X-ray energy-dispersive spectroscopy (EDX). The dendrite trunks lengths of the leaf-like Fe-Ni alloy were about 2.0 μm -8.5 μm , and those of the branch trunk ranged from 850.0 nm to 4.0 μm . Furthermore, it was founded that the formation of leaf-like Fe-Ni alloy strongly depended on the reaction temperature. Moreover, the magnetic and microwave absorption properties of products with various morphologies were also compared, and the result showed that the leaf-like Fe-Ni alloy had higher ferromagnetic and microwave absorption properties compared with spherical Fe-Ni alloy. Copyright © 2013 VBRI Press.

Keywords: Fe-Ni alloy; leaf-like; hydrothermal approach; magnetic properties; microwave absorption properties.

Introduction

Over the past few years, controlling the size and shape of inorganic crystals has attracted significant interest due to the fact that the shape and size of materials have much influence on their chemical and physical properties [1-2]. For example, spray forming technique was employed to produce a near net-shape disc of Al-Si-Pb alloys [3]. The ultrasonic properties of the hexagonal closed packed structured Ag-Zn alloys were studied at room temperature [4]. The semi-solid stirring brazing process of SiCp/A356 composites and 2024 aluminum alloy was reported [5]. Especially, among a variety of inorganic particles, Fe-Ni alloy have been the subject of increasing interest due to their electrical, catalytic and magnetic properties and potential technological applications in catalysis, sensors, electromagnetic shielding and absorbing materials, and so forth [6]. Therefore, it is important to synthesize Fe-Ni alloy with special structures, which may widen its application in various fields. To date, well-defined nanostructures of Fe-Ni alloy with different dimensionalities such as spherical nanoparticles [7-8], triangular particles [9], rods [10], tubes [10-11] nanowires [12-13], nanochains [14] and flowerlike particles [15] have been obtained successfully by a variety of methods. However, these processes usually require complex precursors and/or surfactants. To the best of our knowledge, such reagents not only increase production costs, but also introduce impurities, resulting in noticeable

declines in the properties of the structures. Thus, the development of simple and reliable routes independent of surfactants or complex precursors for the large-scale preparation of pure phase FeNi superstructures remains challenging to researchers. In addition to this, leaf-like magnetic particles are expected to be high microwave absorption properties [16]. Unfortunately, studies on the preparation and microwave absorption properties of leaf-like FeNi are few.

In the current study, we use a hydrothermal approach to prepare leaf-like Fe-Ni superstructures without surfactants and complex precursors. Compared to the reported literatures [7-14], the product in this method is low-cost, high purity and good quality. The morphologies of the products can be conveniently achieved by controlling the reaction temperature. At the same time, magnetic and microwave absorption properties of leaf-like Fe-Ni alloy were also investigated, which is expected to apply in microwave absorption, magnetic and sensing nanodevices.

Experimental

Chemicals

The chemicals used in the experiments are ferric chloride ($\text{FeCl}_3 \cdot 6\text{H}_2\text{O}$) (Shanghai Chemical Reagents Company, 99.7%, Shanghai of China), nickel (II) chloride ($\text{NiCl}_2 \cdot 6\text{H}_2\text{O}$) (Shanghai Chemical Reagents Company, 99.7%, Shanghai of China), sodium hydroxide (Shanghai

Chemical Reagents Company, 99.7%, Shanghai of China), ethanol (Shanghai Chemical Reagents Company, 99.7%, Shanghai of China) and hydrazine hydrate (Shanghai Chemical Reagents Company, 99.7%, Shanghai of China). All chemicals were used without further purification.

Preparation of products

In a typical procedure, 0.71g $\text{NiCl}_2 \cdot 6\text{H}_2\text{O}$ and 0.27g $\text{FeCl}_3 \cdot 6\text{H}_2\text{O}$ were dissolved in 22.5ml ethanol/water (3:1) mixing solution. Subsequently, 7.5ml hydrazine hydrates solution (85%) containing 2.0g NaOH was added into above solution as a reducing agent. The mixture was stirred vigorously and then was transferred into a Teflon cup in a stainless steel-lined autoclave. The autoclave was maintained for 2 h at various reaction temperatures (125°C, 150°C and 180°C) and then was cooled down to room temperature. A black fluffy solid product was deposited on the bottom of the Teflon cup, indicating the formation of Fe-Ni alloys. The final product was collected by a magnet and rinsed with distilled water and ethanol several times to remove any salts, and then dried in a vacuum oven at 40°C for 6 h.

Characterization

The X-ray diffraction (XRD) patterns of the samples were recorded with a Rigaku D/Max-2000 diffractometer equipped with a Cu KR radiation source ($\lambda=0.15418\text{nm}$). The scanning range was from 20° to 80° and the scanning interval was 0.5° . Morphologies of the samples were studied by a Hitachi SU-1500 Scanning electron microscope (SEM). The element composition was characterized by a Horiba EX-250 X-ray energy-dispersive spectrometer (EDX) associated with SEM.

The hysteresis loops were conducted by using a Model-4HF vibrating sample magnetometer at room temperature with a maximum magnetic field of 10kOe. For magnetization measurements, the powder was pressed strongly and fixed in a small cylindrical plastic box. Microwave absorption properties of products were determined using microwave vector network analyser Anritsu Angilent N5230 from 0.5 to 6.0GHz. The cylindrical toroidal samples, with a 3.0mm inner diameter, 7.0mm outer diameter and a thickness of 3.0-3.5mm, were fabricated by uniformly mixing wax with the absorbents in mass ratio of 2:1 and then pressed into cylindrical compacts.

Results and discussion

The formation of leaf-like Ni-Fe alloy was confirmed by the SEM image and EDX spectroscopy as shown in **Fig. 1**. The SEM image in **Fig. 1A** shows that the products consist entirely of such leaf-like structures, indicating the high yield and good uniformity of the leaf-like products prepared by this approach. At the same time, it shows that the leaf-like morphology with a pronounced trunk consists of corrugations and highly ordered branches distributed on both sides of the trunk. The lengths of the dendrite trunks are about 2.0-8.5 μm , and those of the branch trunk range from 850.0nm to 4.0 μm . This is largely different from the

previous reports, in which the nanospheres, polycrystalline nanorods and flower-like Fe-Ni alloy were obtained [**15**, **17-18**]. Moreover, 0.18g leaf-like products is close to the theoretical value of 0.21g calculated by the $\text{NiCl}_2 \cdot 6\text{H}_2\text{O}$ and $\text{FeCl}_3 \cdot 6\text{H}_2\text{O}$ precursor, and the high yield (ca. 86%) is obtained. To further confirm the formation of Fe-Ni alloy, **Fig. 1B** shows the EDX analyses of the leaf-like products. Obviously, both Fe and Ni peaks appear [**15**], and the atomic percentage of Ni is measured to be 74.2% of the sum of Fe and Ni atoms, which is close to the theoretical value of 75% calculated by the $\text{NiCl}_2 \cdot 6\text{H}_2\text{O}$ and $\text{FeCl}_3 \cdot 6\text{H}_2\text{O}$ precursor. This proves that Ni(II) and Fe(III) salts are almost reduced to zerovalent metals. No impurity peak is found in the product. These results indicate that this leaf-like $\text{Ni}_{74.2}\text{-Fe}_{25.8}$ alloy with high yield and purity is prepared by the modified hydrothermal approach.

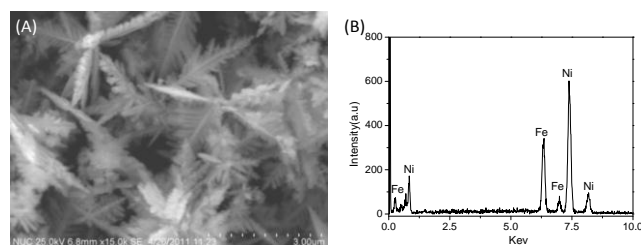


Fig. 1. (A) SEM image and (B) EDX of products prepared at 150°C for 2h.

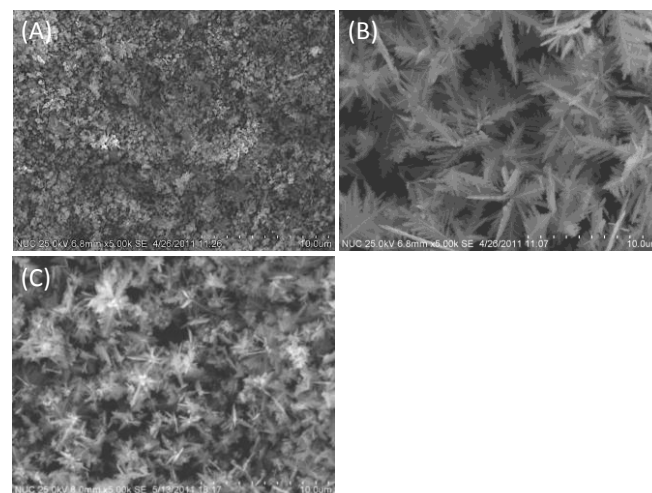


Fig. 2. SEM images of products prepared at various reaction temperatures of (A) 125°C, (B) 150°C and (C) 180°C.

It is further found that the formation and size of the leaf-like Fe-Ni alloy is strongly affected by the reaction temperature. As shown in **Fig. 2A**, the products exhibit spherical morphology with average diameter of about 300.0nm at 125°C, in which some leaf-like Fe-Ni alloy are also observed. As being prepared at 150°C, the spherical particles completely transferred into leaf-like Ni-Fe alloy with average lengths of dendrite trunks (ca. 6.5 μm) and branch trunk (ca. 2.5 μm) as shown in **Fig. 2B**. As shown in **Fig. 2C**, when the reaction temperature is about 180°C, the average lengths of dendrite and branch trunk of leaf-like Ni-Fe alloy decreases from 6.5 μm to 1.5 μm and

2.5 μm to 900.0nm, respectively. These results indicate that the reaction temperature strongly affects the morphology of Ni-Fe alloy. In the other way, the higher temperature (>125 $^{\circ}\text{C}$) do not seem to be responsible for the changes in the morphology of the Ni-Fe alloy, but the size of leaf-like Ni-Fe alloy is affected by the reaction temperature.

The XRD pattern of products prepared at various reaction temperatures was also characterized as shown in Fig.3. It clearly shows three distinctive diffraction peaks at 2θ of 43.8 $^{\circ}$, 51.1 $^{\circ}$ and 75.6 $^{\circ}$, corresponding to (111), (200) and (220) planes of Fe-Ni alloy [14], respectively. No impurity peak is found in the XRD pattern of products. These results further indicate that the leaf-like products with high purity can be prepared by the simple method. At the same time, the result also indicates that the effect of reaction temperature on the formation of Fe-Ni alloy is slight in the present temperature range.

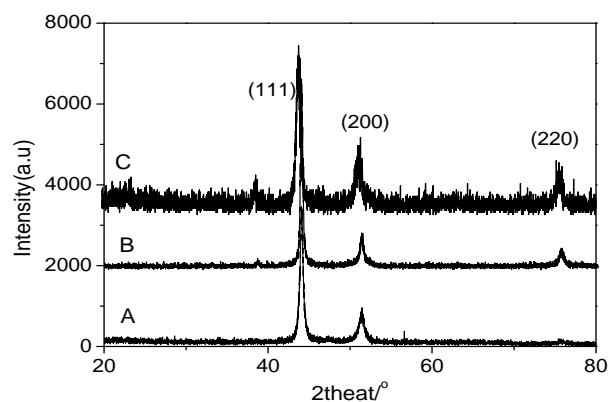


Fig. 3. XRD of products prepared at various reaction temperatures of (A) 125 $^{\circ}\text{C}$, (B) 150 $^{\circ}\text{C}$ and (C) 180 $^{\circ}\text{C}$.

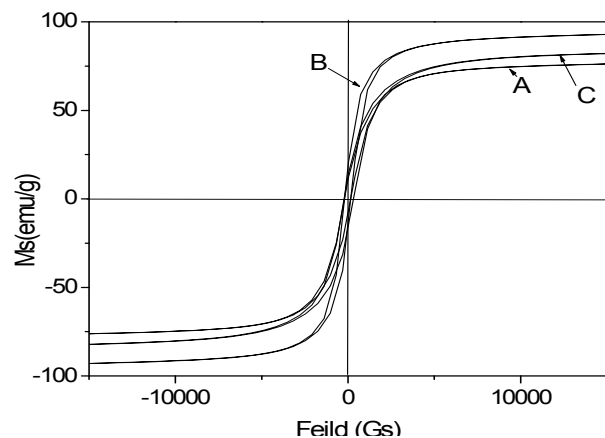


Fig. 4. VSM of products prepared at various reaction temperatures (A) 125 $^{\circ}\text{C}$, (B) 150 $^{\circ}\text{C}$ and (C) 180 $^{\circ}\text{C}$.

The M-H loops of products prepared at various reaction temperatures were further compared as shown in Fig. 4. The hysteresis loops of as-obtained samples exhibit typical ferromagnetic behavior. And the saturation magnetization (M_s) and coercivity (H_c) of all samples are concluded in Table 1. It shows the high M_s of 76.5emu/g, 93.5emu/g and 82.5emu/g for the products prepared at 125 $^{\circ}\text{C}$, 150 $^{\circ}\text{C}$ and 180 $^{\circ}\text{C}$, respectively, which is higher than that (<70.0emu/g) of Fe-Ni alloy in previous works [7-11, 19-20]. The result is attributed to a larger size and more Fe

atomic percentage (25%). Moreover, despite the same composition, the M_s of the leaf-like Fe-Ni alloy (93.5emu/g and 82.5emu/g) is higher than that of the spherical samples. Generally, the M_s of Fe-Ni alloy highly depends on the shape and crystalline anisotropy [21]. The remarkable anisotropic shape of leaf-like Fe-Ni alloy is a major contribution to the enhancement of M_s . On the other hand, the saturation magnetization (M_s) and coercivity (H_c) of the leaf-like Fe-Ni alloy in the work decrease and increase with increase in size, respectively, which is consistent with those of other magnetic particles in previous works [22-23].

Table 1. Saturation magnetization (M_s) and coercivity (H_c) of products prepared by hydrothermal approach

Sample	125 $^{\circ}\text{C}$	150 $^{\circ}\text{C}$	180 $^{\circ}\text{C}$
H_c (Gs)	180.9	180.5	215.7
M_s (emu/g)	76.5	93.5	82.5

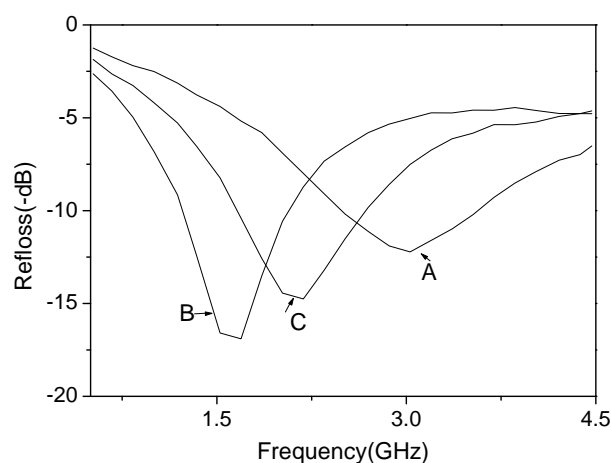


Fig. 5. The reflection loss of Fe-Ni alloy prepared at various reaction temperatures (A) 125 $^{\circ}\text{C}$, (B) 150 $^{\circ}\text{C}$ and (C) 180 $^{\circ}\text{C}$.

Reflection losses (RL) of the Fe-Ni/wax specimens were further investigated as shown in Fig. 5. It can be seen that the RL of products prepared at 125 $^{\circ}\text{C}$, 150 $^{\circ}\text{C}$ and 180 $^{\circ}\text{C}$ is -12.2dB, -16.9dB and -14.8dB, respectively, which is higher than that of Fe-Ni reported in previous works [24-25]. These results indicate that the microwave absorption properties of Fe-Ni are strongly affected by their morphologies and sizes.

In addition to this, large leaf-like Fe-Ni alloy show high microwave absorption properties (ca.-16.9dB), indicating that the leaf-like Fe-Ni alloy is a good kind of microwave absorption materials. The excellent absorption properties of leaf-like Fe-Ni alloy are ascribed to following factors: First, links between leaf-like particles, which form continuous microworlds, may generate a large-scale vibrating micro current; Second, leaf-like superstructures randomly distributed in the matrix can exhibit multiple scattering and further increase the attenuation of the electromagnetic wave; Third, leaf-like superstructures can act as isotropic quasi-antennas, favoring the penetration of electromagnetic

waves into the composites containing leaf-like superstructures. This electromagnetic energy is further induced into a dissipative current and consumed in discontinuous.

Conclusion

In summary, leaf-like Fe-Ni alloy (25% Fe) composed of needle was prepared by a facile modified hydrothermal process without any template. The reaction temperature plays a key role in the formation of leaf-like microstructures. Comparing with the Fe-Ni alloy in previous work, the leaf-like Fe-Ni alloy exhibits enhanced ferromagnetic behavior. The higher saturation magnetization and coercivity comes from the larger size and more Fe atomic percentage (25%) of the sum of Fe and Ni atoms. Moreover, the high microwave absorption properties (ca.-16.9dB) of leaf-like Fe-Ni alloy are also observed. It makes them promising candidates for the design and fabrication of new functional nanomaterials applied in microwave absorption, magnetic and sensing nanodevices.

Acknowledgments

The authors are grateful for the support by National Natural Science Foundation of China under grants (11090330, 11090331 and 11072003) and by the National Basic Research Program of China (G2010CB832701). The China Postdoctoral Science Foundation (2012M510269) and University's Science and technology exploitation of Shangxi Province (20121010) is also acknowledged.

Reference

1. Y. Cui, C. M. Lieber, Functional Nanoscale Electronic Devices Assembled Using Silicon Nanowire Building Blocks, *Science*. 2001, 291, 851-853.
2. Y. Sun, Y. Xia, Shape-Controlled Synthesis of Gold and Silver Nanoparticles, *Science*. 2002, 298, 2176-2179.
3. R. Mittal, A. Tomar, D. Singh, Thickness uniformity and microstructure of disc shape spray formed Al-Si-Pb alloys, *Adv. Mat. Lett.* 2012, 3(1), 55-63.
4. P. K. Yadawa, Behaviour of ultrasonic velocities and elastic constants in Ag-Zn alloys, *Adv. Mat. Lett.* 2011, 2(2), 157-162.
5. H.X. Xu, H. Yang, Q.X. Luo, Y.L. Zeng, B.F. Zhou, C.H. Du, Strength and microstructure of semi-solid stirring brazing of SiCp/A356 composites and aluminum alloy in air, *Adv. Mat. Lett.* 2011, 2(3), 233-238.
6. L. Wang, D.L. Li, M.T. Koike, S. Koso, Y. Nakagawa, Y. Xu, K. Tomishige, Catalytic performance and characterization of Fe-Ni catalysts for the steam reforming of tar from biomass pyrolysis to synthesis gas, *Applied Catalysis A: General*. 2011, 392, 248-255.
7. L. Zhen, Y. X. Gong, J. T. Jiang, W. Z. Shao, Electromagnetic properties of FeNi alloy nanoparticles prepared by hydrogen-thermal reduction method, *Journal of Applied Physics*. 2008, 104, 0343121-0343125.
8. J. Lik, H. Chau, Synthesis of Ni and bimetallic FeNi nanopowders by microwave plasma method, *Materials Letters*. 2007, 61, 2753-2756.
9. D. X. Niu, X. Zou, J. Wu, Y. B. Xu, Anisotropic magnetization reversal in 30 nm triangular FeNi dots, *Applied Physics Letters*. 2009, 94, 0725011-0725013.
10. S.H. Xue, M. Li, Y.H. Wang, X.M. Xu, Electrochemically synthesized binary alloy FeNi nanorod and nanotube arrays in polycarbonate membranes, *Thin Solid Films*. 2009, 517, 5922-5926.
11. D. Zhou, L.H. Cai, F. S. Wen, F. S. Li, Template Synthesis and Magnetic Behavior of FeNi Alloy Nanotube Arrays, *Chinese Journal of Chemical Physics*. 2007, 20, 821-825.
12. R.T. Lv, F.Y. Kang, D.Y. Cai, C. Wang, J. L. Gu, K. L. Wang, D. H. Wu, Long continuous FeNi nanowires inside carbon nanotubes: Synthesis, property and application *Journal of Physics and Chemistry of Solids*. 2008, 69, 1213-1217.
13. A. O. Adeyeye, J. A. C. Bland, C. Daboo, Jaeyong Lee, U. Ebels, H. Ahmed, Size dependence of the magnetoresistance in submicron FeNi

wires, *J. Appl. Phys.* 1996, 79, 6120-6122.

14. J.C. Jia, J. C. Yu, Y.X. J. Wang, K. M. Chan, Magnetic Nanochains of FeNi₂ Prepared by a Template-Free Microwave-Hydrothermal Method, *Applied Materials and Interface*. 2010, 2, 2579-2584.
15. L.J. Liu, J.G. Guan, W.D. Shi, Z.G. Sun, J.S. Zhao, Facile Synthesis and Growth Mechanism of Flowerlike Fe-Ni Alloy Nanostructures, *J. Phys. Chem. C*. 2010, 114, 13565-13570.
16. G. X. Tong, J.H. Yuan, W.H. Wu, Q. Hu, H.S. Qian, L.C. Li, J.P. Shen. Flower-like Co superstructures: Morphology and phase evolution mechanism and novel microwave electromagnetic characteristics, *Cryst Eng Comm*. 2012, 14, 2071-2079.
17. X. W. Wei, G. X. Zhu, J. H. Zhou, H. Q. Sun, Solution phase reduction to Fe-Ni alloy nanostructures with tunable shape and size, *Mater. Chem. Phys.* 2006, 100, 481-485.
18. U. Lačnjevac, B.M. Jović, V.D. Jović, Morphology and composition of the Fe-Ni powders electrodeposited from citrate containing electrolytes, *Electrochimica Acta*. 2009, 55, 535-543.
19. S. Bai, X.P. Shen, G.X. Zhu, Z. Xu, J. Yang, In situ growth of FeNi alloy nanoflowers on reduced graphene oxide nanosheets and their magnetic properties, *Cryst Eng Comm*. 2012, 14, 1432-1438.
20. A. Azizia, Worthwhile effects of salt-matrix reduction on shape, morphology and magnetic properties of FeNi nanoparticles, *Materials Science and Engineering B*. 2011, 176, 1517-1520.
21. R. Ferrando, J. Jellinek, R. L. Johnston, From Theory to applications of alloy clusters and nanoparticles, *Chem. Rev.* 2008, 108, 845-910.
22. Y.Y. Sun, G.Z. Guo, B.H. Yang, W. Cai, Y. Tian, M.H. He, Y.Q. Liu, One-step solution synthesis of Fe₂O₃ nanoparticles at low temperature, *Physica B: Condensed Matter*. 2011, 406, 1013-1016.
23. Y.Y. Sun, X. Zhou, Y.Q. Liu, G.Z. Zhao, Y. Jiang. Effect of magnetic nanoparticles on the properties of magnetic rubber, *Materials research Bulletin*, 2010, 45, 878-881.
24. Y. B. Feng, T. Qiu, Enhancement of electromagnetic and microwave absorbing properties of gas atomized Fe-50wt% Ni alloy by shape modification, *Journal of Magnetism and Magnetic Materials*. 2012, 324, 2528-2533.
25. L. Zhen, Y. X. Gong, J. T. Jiang, W. Z. Shao, Electromagnetic properties of FeNi alloy nanoparticles prepared by hydrogen-thermal reduction method. *Journal of Applied Physics*, 2008, 104, 034312(1-5).

Advanced Materials Letters

Publish your article in this journal

ADVANCED MATERIALS Letters is an international journal published quarterly. The journal is intended to provide top-quality peer-reviewed research papers in the fascinating field of materials science particularly in the area of structure, synthesis and processing, characterization, advanced-state properties, and applications of materials. All articles are indexed on various databases including DOI and are available for download for free. The manuscript management system is completely electronic and has fast and fair peer-review process. The journal includes review articles, research articles, notes, letter to editor and short communications.

